Journal of Alloys and Compounds 509 (2011) 9329–9334

Contents lists available at ScienceDirect

Journal of Alloys and Compounds

journal homepage: www.elsevier.com/locate/jallcom

Enhancement of electron field emission of vertically aligned carbon nanotubes by nitrogen plasma treatment

B.B. Wang[a,b], Q.J. Cheng[b,c], X. Chen[d], K. Ostrikov[b,c,*]

[a] College of Chemistry and Chemical Engineering, Chongqing University of Technology, 69 Hongguang Rd, Lijiatuo, Banan District, Chongqing 400054, PR China
[b] Plasma Nanoscience Centre Australia (PNCA), CSIRO Materials Science and Engineering, P.O. Box 218, Lindfield, NSW 2070, Australia
[c] Plasma Nanoscience, School of Physics, The University of Sydney, Sydney, NSW 2006, Australia
[d] College of Materials Science and Engineering, Chongqing University, Chongqing 400044, PR China

ARTICLE INFO

Article history:
Received 26 May 2011
Received in revised form 3 July 2011
Accepted 7 July 2011
Available online 21 July 2011

PACS:
61.46.+w
79.70.+q

Keywords:
Plasma nanoscience
Plasma made nanostructures
Carbon nanotubes

ABSTRACT

The electron field emission (EFE) characteristics from vertically aligned carbon nanotubes (VACNTs) without and with treatment by the nitrogen plasma are investigated. The VACNTs with the plasma treatment showed a significant improvement in the EFE property compared to the untreated VACNTs. The morphological, structural, and compositional properties of the VACNTs are extensively examined by scanning electron microscopy, transmission electron microscopy, Raman spectroscopy, and energy dispersive X-ray spectroscopy. It is shown that the significant EFE improvement of the VACNTs after the nitrogen plasma treatment is closely related to the variation of the morphological and structural properties of the VACNTs. The high current density (299.6 $\mu A/cm^2$) achieved at a low applied field (3.50 $V/\mu m$) suggests that the VACNTs after nitrogen plasma treatment can serve as effective electron field emission sources for numerous applications.

1. Introduction

Low-dimensional carbon-based nanomaterials have attracted increasing interest owing to their remarkable mechanical, physical, chemical, and electrical properties [1–8]. For example, graphene, a one atom thick quasi-two dimensional material made up of sp^2-bonded carbon atoms densely packed in a honeycomb crystal lattice, features an extremely high room-temperature electron mobility of approximately 15,000 $cm^2\,V^{-1}\,s^{-1}$, an ultra-low resistivity of $10^{-6}\,\Omega\,cm$ as well as a remarkable high opacity with an absorption ratio of only approximately 2% of white light [8–11]. Another example is that carbon nanotubes (CNTs) can be either metallic or semiconducting depending on the chirality, diameter, and wall number [1,3,5,8]. In particular, due to their high aspect ratio and small tip radius, CNTs are very suitable as electron field emission (EFE) sources for applications in the areas of flat panel displays, atomic force microscope probes, sensors, etc. [1–5,12–18].

In order to maximize the field emission current density and simultaneously minimize the emission turn-on voltage, the EFE characteristics of CNTs have been extensively investigated. However, a detailed understanding of the emission behavior of the CNTs is still far from complete. This is because the emission behavior of the CNTs is rather sensitive to various properties, including but not limited to morphology, structural defects, bonding states, diameter and density, as well as the intertube distance [2,19,20]. For example, Park et al. [19] found that the vertically aligned carbon nanotubes (VACNTs) showed inferior EFE characteristics compared with carbon nanoclusters. Another example is that Nilsson et al. [20] reported that the EFE characteristics of bent CNTs depended on the density of CNTs and that high-density CNTs exhibited relatively poor EFE characteristics. They also pointed out that the poor EFE characteristics of the high-density CNTs were attributed to the electrostatic screening effect due to the proximity of neighboring tubes [19,20].

Recently, to further improve the electron field emission characteristics of CNTs, a variety of surface treatment approaches have been proposed, such as gas adsorption, electron radiation, ion bombardment, plasma treatment and chemical modification [21–25]. For instance, Zhi et al. [23] and Gohel et al. [24] exposed synthesized random multi-walled carbon nanotubes to hydrogen and nitrogen plasmas, respectively, and found that the EFE characteristics could be improved by plasma treatment. In addition, Chen et al. [25] reported that the turn-on field of CNTs decreased from 1.8 to 0.8 $V/\mu m$ after deposition of IrO_2 on the CNT surfaces. However, only very few research efforts have been focused on the investigation of field emission behavior of well-aligned CNTs after

* Corresponding author at: Plasma Nanoscience, School of Physics, The University of Sydney, Sydney, NSW 2006, Australia. Tel.: +61 02 9413 7634; fax: +61 02 9413 7200.
E-mail address: kostya.ostrikov@csiro.au (K. Ostrikov).

0925-8388/$ – see front matter.
doi:10.1016/j.jallcom.2011.07.026

the plasma treatment. In our previous work, the effect of oxygen adsorption on the EFE characteristics of VACNTs was studied [26]. In this work, we focus on studying the effect of nitrogen plasma treatment on the EFE characteristics of VACNTs. We also show that the EFE characteristics of VACNTs are closely related to the variation of the nanotube morphology and structure after the nitrogen plasma treatment.

2. Experimental details

The vertically aligned carbon nanotubes were grown on (1 0 0) single-crystal silicon substrates pre-deposited with a 50-nm-thin titanium film as a buffer layer and a 40 nm nickel film as a catalyst layer using a custom-designed bias-enhanced hot-filament chemical vapor deposition reactor. The details of the deposition system and its operation can be found elsewhere [27]. Briefly, the reactor contains three coiled hot tungsten filaments for feedstock gas heating and pre-ionization. The distance from the substrate to the filaments was about 8 mm. A DC bias was applied to the substrate to draw the ion flux toward the specimens and sustain the plasma discharge by enhancing the ionization of the feedstock gas. Prior to the deposition, a base pressure of approximately 3×10^{-2} Torr was achieved through the use of a rotary pump. Thereafter, high-purity (99.999%) methane, ammonia and hydrogen gases with flow rates of 20, 10, and 70 sccm (sccm denotes cubic centimeters per minute at standard temperature and pressure), respectively, were introduced into the chamber, whereupon the total working gas pressure was maintained at 10^3 Pa. The filament was then heated to about 1600 °C and the substrate surface temperature was estimated to be approximately 650 °C (measured using a thermocouple). Later, a bias power with the bias current setting at 180 mA was switched on to produce a plasma and maintained for 30 min for the growth of VACNTs.

To study the effect of nitrogen plasma treatment on the electron field emission characteristics of the VACNTs, the sample was cut into two segments: one was treated with nitrogen plasma, and the other was kept unaltered as a reference. For the nitrogen plasma treatment experiments, the flow rate and pressure of nitrogen were 50 sccm and 700 Pa, respectively. The substrate temperature was about 450 °C and the bias current was set to 100 mA with a treatment time of 1.5 min.

The EFE characteristics of the VACNTs were measured using a diode configuration in a vacuum system of $\sim 10^{-6}$ Pa. In the diode configuration, the VACNT film was used as the cathode and a mirror-polished silicon wafer was used as the anode, and they were separated by a polyimide film with a thickness of 28 μm. During the measurement process, the voltage was changed from 1 to 160 V.

The structural, morphological, and compositional properties of the VACNTs were investigated by scanning electron microscopy (SEM), transmission electron microscopy (TEM), energy dispersive X-ray (EDX) spectroscopy, and Raman spectroscopy. SEM measurements were performed using a Hitachi S-4800 field emission scanning electron microscope. EDX measurements were carried out by EX-350 EDX spectrometer (coupled to the SEM). TEM measurements were undertaken by Philips CM120 Biofilter (operated at 120 kV) transmission electron microscope. The specimens for TEM imaging were prepared by suspending solid samples in ethanol. About 1–2 mg of solid sample detached from the Si substrate was added to 5 mL of ethanol in a small glass vial, followed by sonication for 5 min. A few drops of the sonicated suspension were dropped onto a carbon-coated 200 mesh copper grid and dried under ambient conditions before imaging. Raman measurements were conducted by a Renishaw micro-Raman system using a 514.5 nm Ar^+ laser for excitation.

3. Results

Fig. 1(a)–(b) shows typical SEM images of the VACNTs before and after the nitrogen plasma treatment. As shown in Fig. 1(a), the as-grown VACNTs feature high density and are uniformly distributed throughout the whole substrate. The average diameter and length of the VACNTs deduced from Fig. 1(a) are ~45 nm and ~1.18 μm, respectively. Moreover, one can also notice some disordered carbon material and/or contamination. After 1.5 min of the nitrogen plasma treatment, the disordered carbon material and/or contamination are effectively etched away from the surface of the VACNTs and the nanotube length slightly decreases. This is presumably due to the surface bombardment by the nitrogen-based ions (in nitrogen plasmas, a molecular ion N_2^+ is usually more abundant than N^+) or other plasma–surface interactions. The clean surface of the VACNTs after the nitrogen plasma treatment is beneficial for the carbon nanotube field emission characteristics [23,24].

Fig. 2(a)–(b) shows typical TEM micrographs of the individual nanotubes before and after the nitrogen plasma treatment. Before the plasma treatment, the nanotubes feature multiple straight walls as can be seen in Fig. 2(a). Their structure, however, changes

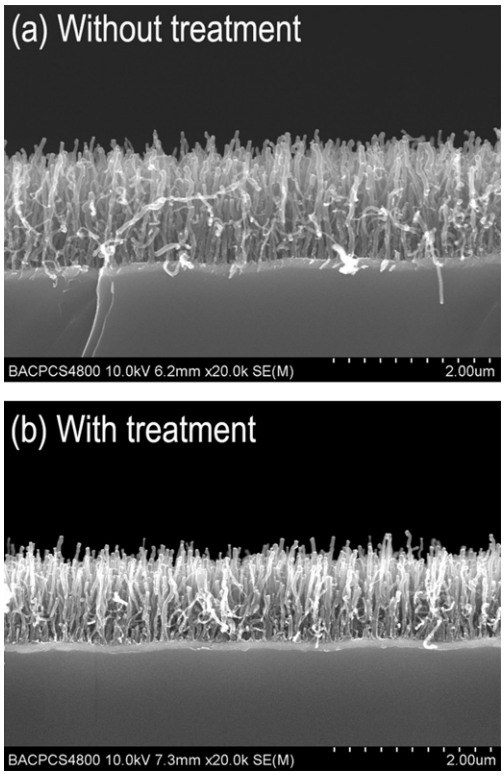

Fig. 1. Typical SEM images of the VACNTs before (a) and after (b) the nitrogen plasma treatment.

after the plasma treatment. One can notice from Fig. 2(b) that the individual VACNT is a bamboo-structured multiwall CNT with a pear-shaped Ni particle on the tip. This structure is also commonly referred as a carbon nanofiber [28,29]. The formation of bamboo-structured multiwall CNTs indicates that nitrogen atoms are incorporated into the VACNTs, which was explained in detail in our previous work [30]. One can also notice that the tip of the Ni particle is slightly etched, most likely due to the interaction with nitrogen-based ions. This is advantageous for the electron field emission because nanotubes with small catalyst particles can enhance the local electron field near the top [23].

Fig. 3 presents the Raman spectra recorded from the VACNTs without and with treatment by the nitrogen plasma. As one can see in Fig. 3, there are two main D and G peaks which are located at 1353 and 1581 cm^{-1} in spectrum (1) for the VACNTs without the plasma treatment; while these two main D and G peaks are found at 1354 and 1591 cm^{-1} in spectrum (2) for the VACNTs after the nitrogen plasma treatment. It is generally believed that the D peak is related to the A_{1g} breathing mode which is attributed to the defects in a graphite sheet, sp^3 carbon clusters, or other impurities; while the G peak is attributed to the $E_{2g}{}^{(2)}$ mode which corresponds to the movement of two neighboring carbon atoms in opposite directions within the crystalline or ordered graphene sheet [12,31,32].

It is noteworthy that the G peak is shifted from 1581 to 1591 cm^{-1} after the VACNTs were treated with nitrogen plasmas. This shift originates from the incorporation of nitrogen atoms into the carbon sheets of the VACNTs because the electronic structure of CNTs is modified with nitrogen incorporation [33]. This result is consistent with the TEM analysis in Fig. 2. The ratio of the intensities of the D peak to the G peak can be used to estimate the relative content of structural defects [12,31]. Deduced from Fig. 3, the ratios of the intensities of the D peak to the G peak of the nanotubes without and with the nitrogen plasma treatment are 1.12 and 1.22, respectively. The increased ratio of the intensities of the D peak to

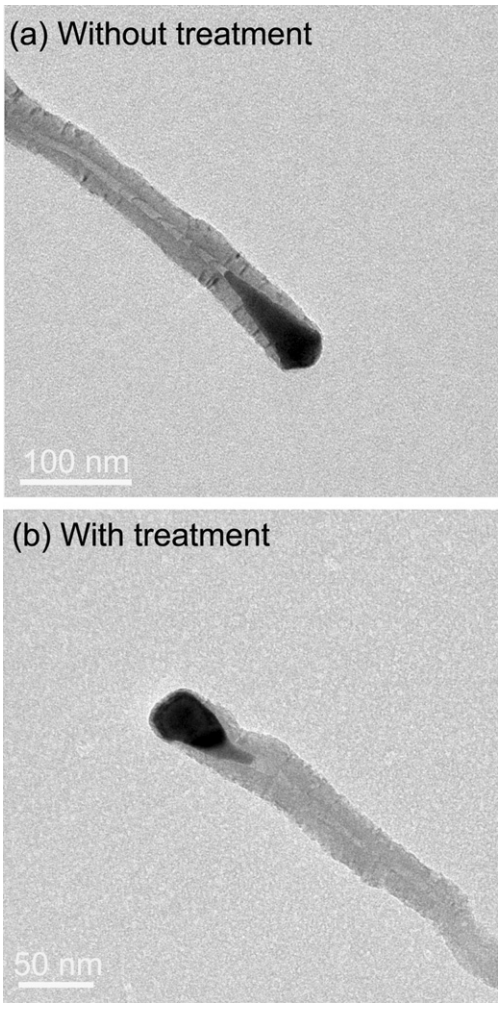

Fig. 2. Typical TEM micrographs of the individual nanotubes before (a) and after (b) the nitrogen plasma treatment.

the G peak with the treatment by the nitrogen plasma indicates an increase in the nitrogen content or sp^3 carbon content in the VACNTs [31,34].

Fig. 4 displays the EDX spectra of the VACNTs without and with treatment by the nitrogen plasma. The insets show the corresponding weight and atomic elemental concentrations of the carbon nanotubes before and after the nitrogen plasma treatment.

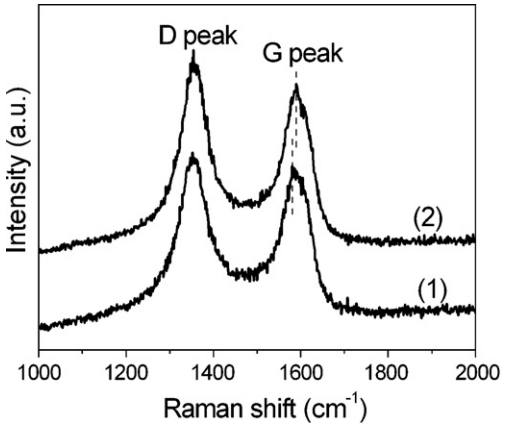

Fig. 3. Raman spectra recorded from the VACNTs without (1) and with (2) treatment by the nitrogen plasma.

As shown in Fig. 4, there is an oxygen signal but there is no nitrogen signal. It is possible that the nitrogen signal is rather weak so that it does not appear in the spectrum. In addition, the appearance of the oxygen signal in Fig. 4 indicates that oxygen molecules can easily be adsorbed on the VACNTs. It is noteworthy that the oxygen and nickel atomic concentrations (shown in the insets) are reduced from 0.87 to 0.76 at.% and from 1.08 to 0.37 at.%, respectively, after the treatment by the nitrogen plasma. The decrease of the oxygen and nickel atomic concentrations in the nanotubes after the nitrogen plasma treatment is attributed to the surface bombardment by the nitrogen-based ions or other plasma–surface interactions as mentioned previously.

Fig. 5(a) shows the typical curves of the field emission current density J versus the applied electric field E for the VACNTs without and with treatment by the nitrogen plasma. It is evident that the field emission performance of the nanotubes is significantly improved after the nitrogen plasma treatment. For example, at an applied electric field of 3.50 V/μm, the emission current density is only 6.7 μA/cm^2 for the as-deposited VACNTs, while the emission current density increases approximately 44 times and reaches a high value of 299.6 μA/cm^2 after the nitrogen plasma treatment. This high current density achieved at a rather low applied electric field suggests that the VACNTs can indeed serve as effective electron field emission sources for numerous applications in flat panel display, electron microscopy, and other advanced technologies.

In order to determine the turn-on field for the VACNTs, we used a similar methodology to that proposed by Chen et al. [35]. The turn-on field is defined as the field where the Fowler-Nordheim (F-N) curve deviates from a straight line [35]. Fig. 5(b) shows the corresponding F-N plots for the VACNTs without and with the nitrogen plasma treatment. One can observe that at a low applied electric field, both F-N curves can be fitted well with a straight line, which suggests that the measured current is determined by the field emission [36]. The turn-on fields deduced from the linear fitting are approximately 1.15 and 0.79 V/μm for the nanotubes without and with treatment by the nitrogen plasma, respectively. The significant reduction of the turn-on field suggests that the electron field emission properties of VACNTs are significantly enhanced after the nitrogen plasma treatment.

4. Discussion

Our experiments suggest that the electron field emission characteristics of the VACNTs are significantly improved after the nitrogen plasma treatment. This may be attributed to the variation of the morphological and structural properties of the nanotubes through the plasma–surface interactions. In this section, we will analyze the effect of the nitrogen plasma on the EFE characteristics of the VACNTs.

4.1. Effect of nitrogen-based ion bombardment

When the VACNTs are treated with the nitrogen plasma, the nitrogen-based species can effectively interact with the nanotubes. These interactions include, but are not limited to: desorption of oxygen molecules from the surface, incorporation of nitrogen atoms into the carbon sheets of the VACNTs, and adsorption of nitrogen molecules on the nanotube surfaces. Before the treatment of the nanotubes with the nitrogen plasma, they were exposed to air. As a result, oxygen molecules were adsorbed on the nanotube surfaces due to the strong affinity of oxygen molecules to VACNTs [37]. During the treatment of the VACNTs by nitrogen plasmas, oxygen molecules are effectively desorbed from the surface of the nanotubes. This is because: (1) the substrate is heated during plasma treatment so that the interaction between oxygen

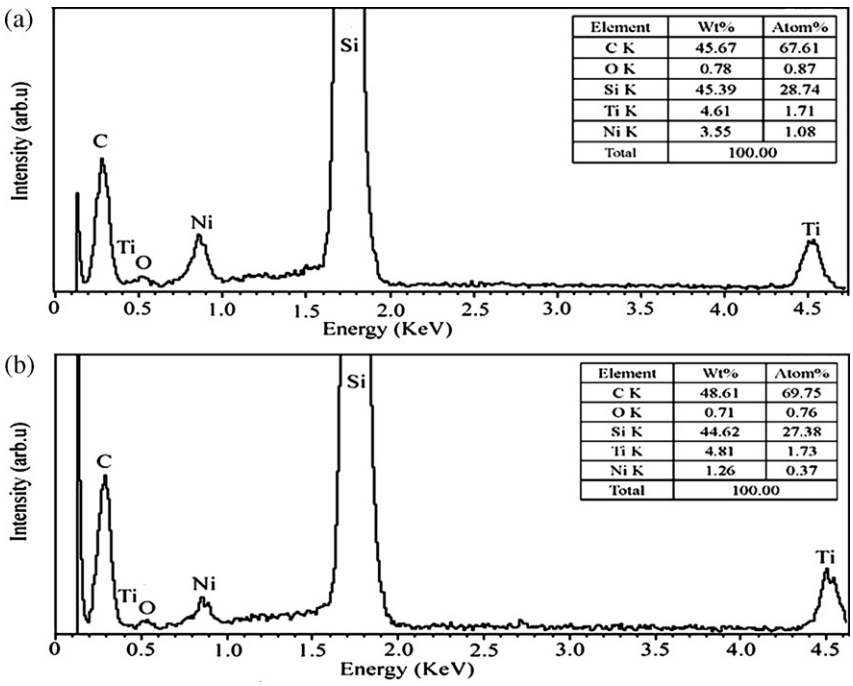

Fig. 4. EDX spectra of the VACNTs without (a) and with (b) treatment by the nitrogen plasma. The insets show the corresponding weight and atomic elemental concentrations of the carbon nanotubes before and after the nitrogen plasma treatment.

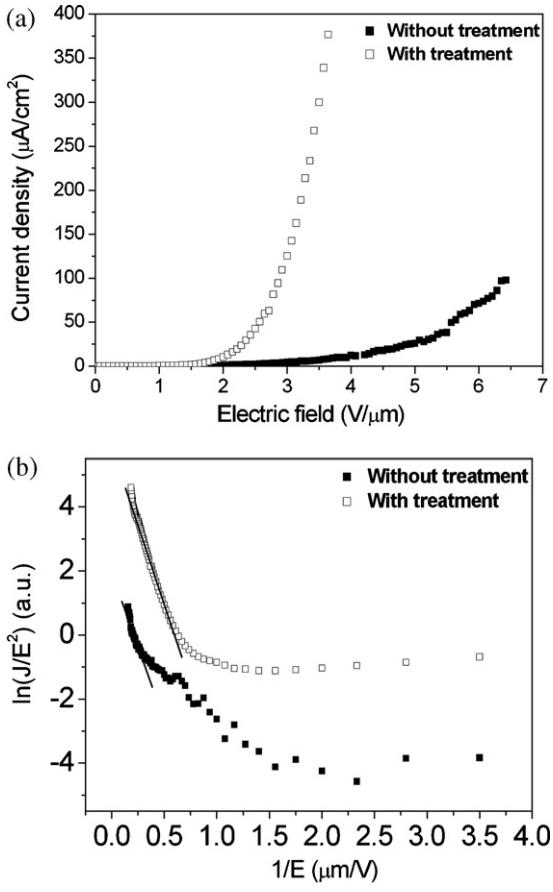

Fig. 5. (a) Typical curves of the field emission current density J versus the applied electric field E for the VACNTs without and with treatment by the nitrogen plasma; (b) corresponding F-N plots for the VACNTs without and with treatment by the nitrogen plasma.

molecules and VACNTs is significantly weakened; (2) nitrogen-based ions produced in the plasma effectively bombard the surface of the VACNTs. This is confirmed by the insets of Fig. 4, which shows that oxygen atomic concentration is reduced after the VACNTs were treated by the nitrogen plasma.

Due to the bombardment effect of nitrogen-based ions, some carbon atoms in the carbon sheets of the VACNTs are sputtered or displaced by some of the nitrogen-based ions whose energy is close to the binding energy of carbon atoms in the carbon sheets [38]. In this case, the nitrogen-based ions are easily incorporated into the carbon sheets of the nanotubes. The incorporation of nitrogen atoms into the carbon sheets is confirmed by the TEM and Raman analysis. The incorporation of nitrogen atoms into multi-walled carbon nanotubes was also reported by Gohel et al. [24]. They pointed out that the incorporation of nitrogen atoms into the carbon nanotubes was favorable for the formation of C–N, C═N and C≡N bonding configurations. When the treatment is completed, the substrate is cooled to room temperature in a nitrogen environment. It is quite likely that nitrogen molecules are then adsorbed on the VACNTs.

4.2. Change in work function of VACNTs

Due to the incorporation of nitrogen atoms into the carbon sheets of the VACNTs, the work function of the nanotubes is reduced. Gohel et al. [24] reported that C═N and C≡N bonding configurations were the main components in the formed carbon nitride if CNTs were processed for 10 and 20 min, respectively. Moreover, the content of carbon nitride with C–N bonding configuration increased with time [24]. For our sample, the treatment time was only 1.5 min. Therefore, the C═N bonding configuration should be the main component of the formed carbon nitride. The results of Terrones et al. [39] indicated that the formation of the C═N bonding configuration in the VACNTs induced donor states close to the Fermi level, which brought about a shift of 0.18 eV of the Fermi level toward the conduction band. Thus, the difference between the vacuum level and the Fermi level decreases by 0.18 eV, and as such the work function is reduced.

When gas molecules are adsorbed on the CNTs, the work function of CNTs also changes depending on the types of gas molecules. Due to the electronegativity difference between elements, there is a charge transfer between the atoms of the gas molecules and carbon atoms after gas molecule or ion adsorption on CNTs. As a result, a dipole layer is formed on the surfaces of CNTs leading to the change in the CNT work function [23,40]. The results of Kim et al. [21] indicated that the adsorption of oxygen and hydrogen molecules on CNTs resulted in the shift of the Fermi level toward the valence and conduction bands, respectively. However, the shift of the Fermi level caused by the adsorption of nitrogen molecules was small. Thus, the adsorption of oxygen molecules on CNTs leads to the increase in the work function of CNTs while the change in the work function due to adsorption of nitrogen molecules appears to be small.

4.3. Interpretation of the electron field emission improvement

Our results suggest that, after the VACNTs are exposed to the nitrogen plasma, the nitrogen-based ions are effectively incorporated into the nanotubes. Moreover, oxygen molecules adsorbed on the surface of the as-deposited VACNTs are effectively desorbed from the surface. Thereby, the work function is reduced due to the incorporation of nitrogen atoms in the CNTs through the effective formation of donor states [39]. In this way, the EFE characteristics of the VACNTs are significantly improved through the bombardment by nitrogen-based ions.

We stress that the significant improvement of the EFE characteristics of the VACNTs after the nitrogen plasma treatment can be attributed to a combination of several factors such as the reduction of work function, the improvement of the phase purity, effective formation of nitrogen doping states, desorption of oxygen molecules on the nanotube surfaces, etching of the top surface of Ni catalyst nanoparticles, as well as some other effects [12,23,24,36].

Finally, it is worthwhile to mention that the plasma-based approach has also been extensively used to enhance the electron field emission of other low-dimensional nanostructures such as nanowires. Two typical strategies have been employed. One strategy is to use plasmas for producing an electric field during the nanowire synthesis [41–43]. This electric field can guide the nanowire growth, resulting in better nanowire vertical alignment, better emitter shapes, etc. [41–43]. For example, Li et al. [41] compared the field emission properties of In_2O_3 nanowires synthesized without and with using plasmas, and showed that the plasma-made In_2O_3 nanowires had lower turn-on and threshold electric fields than the In_2O_3 nanowires synthesized without using plasmas. The other strategy is to post-treat the as-grown nanowires using plasmas to rearrange the position, location, etc. [44,45]. For instance, Zhu et al. [44] showed that the electron field emission performance of the as-grown CuO nanowires was significantly enhanced after the oxygen plasma treatment. They attributed this enhancement to the reduction of the tip diameter of the nanowires, the sharpening of the nanowire tips, and the removal of the amorphous layer on the surface of the as-grown nanowires.

It is noteworthy that, the electric field (produced by the plasma) and plasma treatment time should be at appropriate values for the field enhancement effect of the plasma-made nanostructures [46,47]. This will not affect the synthesis process. However, if the electric field is too high or the plasma treatment time is too long, it will bring about some adverse effects for the synthesized nanostructures such as destroying the nanostructure arrays, change of the crystal structures, etc. Under these conditions, it will affect the synthesis process, which will adversely affect the field emission performance of the synthesized nanostructures [46,47].

5. Conclusions

In summary, the VACNTs were synthesized using a custom-designed bias-enhanced hot filament chemical vapor deposition reactor and then treated by a nitrogen plasma. It is found that the electron field emission characteristics of the VACNTs are significantly improved after the nitrogen plasma treatment. We have further clarified the mechanism of such an improvement in the electron field emission property of the VACNTs. Several factors such as work function, doping state, oxygen adsorption, phase purity, catalyst surface, etc., play roles on the EFE performance of the CNTs. These results are highly relevant to the development of flat panel displays, atomic force microscope probes, sensors, and several other advanced applications.

Acknowledgements

This work is partially supported by the Scientific Research Foundation of Chongqing University of Technology, Chongqing Natural Science Foundation of China (CSTC, 2009BA4027), CSIRO's OCE Science Leadership Scheme, the Australian Research Council, National Natural Science Foundation of China (NSFC, 90923005), and Shanghai Science and Technology Committee (SSTC, 09ZR1414600). We thank A.E. Rider for editing and proofreading the manuscript and fruitful discussions.

References

[1] M.A. Salam, M.S.I. Makki, M.Y.A. Abdelaal, J. Alloys Compd. 509 (2011) 2582–2587.
[2] I. Denysenko, K. Ostrikov, U. Cvelbar, M. Mozetic, N.A. Azarenkov, J. Appl. Phys. 104 (2008) 073301–73309.
[3] M. Keidar, I.I. Beilis, J. Appl. Phys. 106 (2009) 103304–103306.
[4] I. Levchenko, K. Ostrikov, Appl. Phys. Lett. 92 (2008) 063108–63113.
[5] K. Ostrikov, Rev. Mod. Phys. 77 (2005) 489–511.
[6] D.B. Mahadik, S.S. Shinde, C.H. Bhosale, K.Y. Rajpure, J. Alloys Compd. 509 (2011) 1418–1423.
[7] H. Wu, P. Cao, W. Li, N. Ni, L. Zhu, X. Zhang, J. Alloys Compd. 509 (2011) 1261–1265.
[8] K. Ostrikov, U. Cvelbar, A.B. Murphy, J. Phys. D: Appl. Phys. 44 (2011) 174001–174029.
[9] W. Choi, I. Lahiri, R. Seelaboyina, Y.S. Kang, Crit. Rev. Solid State Mater. Sci. 35 (2010) 52–71.
[10] T. Lu, L. Pan, H. Li, G. Zhu, T. Lv, X. Liu, Z. Sun, T. Chen, D.H.C. Chua, J. Alloys Compd. 509 (2011) 5488–5492.
[11] X. Yue, H. Wang, S. Wang, F. Zhang, R. Zhang, J. Alloys Compd. 505 (2010) 286–290.
[12] Z.L. Tsakadze, K. Ostrikov, J.D. Long, K. Ostrikov, Diamond Relat. Mater. 13 (2004) 1923–1929.
[13] K. Ostrikov, H.J. Yoon, A.E. Rider, S.V. Vladimirov, Plasma Proc. Polym. 4 (2007) 27–40.
[14] X. Zhong, X. Wu, K. Ostrikov, Plasma Proc. Polym. 6 (2009) 161–169.
[15] Y. Zhan, L. Pan, C. Nie, H. Li, Z. Sun, J. Alloys Compd. 509 (2011) 5667–5671.
[16] Y.C. Bai, W.D. Zhang, C.H. Chen, J.Q. Zhang, J. Alloys Compd. 509 (2011) 1029–1034.
[17] K.T. Kim, G.H. Ha, J. Eckert, J. Alloys Compd. 509S (2011) S412–S415.
[18] X.S. Liu, F. Hu, D.R. Zhu, D.N. Jia, P.P. Wang, Z. Ruan, C.H. Cheng, J. Alloys Compd. 509 (2011) 2829–2832.
[19] K.H. Park, S. Choi, L.M. Lee, S. Lee, K.H. Koh, J. Vac. Sci. Technol. B 19 (2001) 958–961.
[20] L. Nilsson, O. Groening, C. Emmenegger, O. Kuettel, E. Schaller, L. Schlapbach, H. Kind, J.M. Bonard, K. Kem, Appl. Phys. Lett. 76 (2000) 2071–2073.
[21] C. Kim, Y.S. Choi, S.M. Lee, J.T. Park, B. Kim, Y.H. Lee, J. Am. Chem. Soc. 124 (2002) 9906–9911.
[22] S.C. Lim, Y.C. Choi, H.J. Jeong, Y.M. Shin, K.H. An, D.J. Bae, Y.H. Lee, N.S. Lee, J.M. Kim, Adv. Mater. 13 (2001) 1563–1567.
[23] C.Y. Zhi, X.D. Bai, E.G. Wang, Appl. Phys. Lett. 81 (2002) 1690–1692.
[24] A. Gohel, K.C. Chin, Y.W. Zhu, C.H. Sow, A.T.S. Wee, Carbon 43 (2005) 2530–2535.
[25] Y.M. Chen, C.A. Chen, Y.S. Huang, K.Y. Lee, K.K. Tiong, J. Alloys Compd. 487 (2009) 659–664.
[26] C. Dang, B.B. Wang, F.Y. Wang, Vacuum 83 (2009) 1414–1418.
[27] B.B. Wang, K. Ostrkov, J. Appl. Phys. 105 (2009) 083303–83309.
[28] A.V. Melechko, V.I. Merkulov, T.E. McKnight, M.A. Guillorn, K.L. Klein, D.H. Lowndes, M.L. Simpson, J. Appl. Phys. 97 (2005) 041301–41339.
[29] I. Denysenko, K. Ostrikov, Appl. Phys. Lett. 90 (2007) 251501–251503.
[30] T.Z. Wang, B.B. Wang, Appl. Surf. Sci. 253 (2006) 1606–1610.

[31] C. Chen, A. Ogino, X. Wang, M. Nagatsu, Diamond Relat. Mater. 20 (2011) 153–156.
[32] Q.J. Cheng, S. Xu, J.D. Long, S.Y. Huang, J. Guo, Nanotechnology 18 (2007) 465601–465606.
[33] L.G. Bulusheva, A.V. Okotrub, I.A. Kinloch, I.P. Asanov, A.G. Kurenya, A.G. Kudashov, X. Chen, H. Song, Phys. Status Solidi (b) 245 (2008) 1971–1974.
[34] A. Aitkaliyeva, M.C. McCarthy, M. Martin, E.G. Fu, D. Wijesundera, X. Wang, W.K. Chu, H.K. Jeong, L. Shao, Nucl. Instrum. Methods Phys. Res. B 267 (2009) 3443–3446.
[35] S.C. Chen, L.Y. Shih, Y.C. Chen, G.C. Tu, I.N. Lin, J. Vac. Sci. B 19 (2001) 1026–1029.
[36] Z.L. Tsakadze, K. Ostrikov, C.H. Sow, S.G. Mhaisalkar, Y.C. Boey, J. Nanosci. Nanotechnol. 10 (2010) 6575–6579.
[37] A. Abbas, Z.Y. Wu, J. Zhong, K. Ibrahim, A. Fiori, S. Orlanducci, V. Sessa, M.L. Terranova, I. Davoli, Appl. Phys. Lett. 87 (2005) 051923–51933.
[38] B.B. Wang, B. Zhang, Carbon 44 (2006) 1949–1953.
[39] M. Terrones, P.M. Ajayan, F. Banhart, X. Blase, D.L. Carroll, J.C. Charlier, R. Czerw, B. Foley, N. Grobert, R.K. Kamalakaran, P.K. Redlich, M. Rühle, T. Seeger, H. Terrone, Appl. Phys. A 74 (2002) 355–361.
[40] N.K. Luo, K. Yamaguchi, T. Terai, M.J. Yamawaki, J. Nucl. Mater. 290-293 (2001) 116–120.
[41] S.Q. Li, Y.X. Liang, T.H. Wang, Appl. Phys. Lett. 87 (2005) 143104–143113.
[42] J.G. Lu, P. Chang, Z. Fan, Mater. Sci. Eng. R 52 (2006) 49–91.
[43] Z. Chen, U. Cvelbar, M. Mozetic, J. He, M.K. Sunkara, Chem. Mater. 20 (2008) 3224–3228.
[44] Y.W. Zhu, A.M. Moo, T. Yu, X.J. Xu, X.Y. Gao, Y.J. Liu, C.T. Lim, Z.X. Shen, C.K. Ong, A.T.S. Wee, J.T.L. Thong, C.H. Sow, Chem. Phys. Lett. 419 (2006) 458–463.
[45] J. Joo, S.J. Lee, D.H. Park, Y.S. Kim, Y. Lee, C.J. Lee, S.R. Lee, Nanotechnology 17 (2006) 3506–3511.
[46] C.P. Juan, C.C. Tsai, K.H. Chen, L.C. Chen, H.C. Cheng, Jpn. J. Appl. Phys. 44 (2005) 8231–8236.
[47] K.S. Ahn, J.S. Kim, C.O. Kim, J.P. Hong, Carbon 41 (2003) 2481–2485.